The metamorphic evolution of the Patscherkofel Crystalline Complex (Tyrol, Eastern Alps, Austria)

Andreas PIBER, Peter TROPPER*) & Peter W. MIRWALD

Institute of Mineralogy and Petrography, Faculty of Geo- and Atmospheric Sciences, University of Innsbruck, Innrain 52, A-6020 Innsbruck, Austria.

*) Corresponding author, peter.tropper@uibk.ac.at

KEYWORDS

Patscherkofel Crystalline Complex
Thermobarometry
Eo-Alpine
Austria

Abstract

The Patscherkofel Crystalline Complex (PCC) is part of the Austroalpine basement nappes north of the Tauern Window, which is tectonically located on top of the Innsbruck Quartzphyllite. The PCC is mainly composed of micaschists with the mineral assemblage plagioclase$_{1,2}$ + muscovite + biotite + chlorite + quartz ± chloritoid ± garnet$_{1,2}$ ± ilmenite ± clinozoisite ± staurolite ± margarite. Garnet$_1$ + plagioclase$_1$ + staurolite represent amphibolite-facies pre-Alpine relics, all other minerals are part of the Eo-Alpine mineral assemblage. Application of the garnet – biotite thermometer and the garnet – plagioclase – muscovite – quartz barometer, yields temperatures between 510°C and 570°C and pressures ranging from 9.5 to 12.2 kbar for the samples from the PCC. Thermobarometric calculations with multi-equilibrium programs such as TWQ v.1.02 and THERMOCALC v.3.02 in the H_2O-present system KCNFMASH and the two H_2O-absent systems KCNFMAS and KCFMAS yield pressures in a range of 7.3 – 11.5 kbar and temperatures of 454 – 585°C for the same samples. These *P-T* data can be correlated with geochronological data from the area and thus indicate a strong Eo-Alpine metamorphic overprint. In addition, the *P-T* data of the Eo-Alpine mineral assemblage from the PCC are in good agreement with the southern parts of the Ötztal Complex and thus the PCC most likely represents an eastward extension of the Ötztal Complex, separated from it during the late-stage Alpine extension in the course of the uplift of the Tauern Window.

Das Patscherkofelkristallin (PCC) ist Teil der austroalpinen Basementeinheiten nördlich des Tauernfensters, und befindet sich tektonisch auf dem Innsbrucker Quarzphyllit. Das PCC besteht hauptsächlich aus Glimmerschiefern mit der Paragenese Plagioklas$_{1,2}$ + Muskovit + Biotit + Chlorit + Quarz ± Chloritoid ± Granat$_{1,2}$ ± Ilmenit ± Klinozoisit ± Staurolith ± Margarit. Granat$_1$ + Plagioklas$_1$ + Staurolith stellen noch amphibolitfazielle, prä-alpine Relikte dar. Alle anderen Minerale werden als Teil der eo-alpidischen Mineralparagenese interpretiert. Granat-Biotit-Thermometrie und Granat-Plagioklas-Muskovit-Quarz-Barometrie ergaben *P-T* Bedingungen von 9.5 bis 12.2 kbar und 510 – 570°C. Multi-equilibrium Thermobarometrie (TWQ v.1.02 und THERMOCALC v.3.02) mithilfe des H_2O-führenden Systems KCNFMASH und den H_2O-abwesenden Systemen KCNFMAS und KCFMAS ergab ähnliche *P-T* Bedingungen von 7.3 – 11.5 kbar und 454 – 585°C. Korreliert man diese *P-T* Daten mit den verfügbaren geochronologischen Daten aus diesem Gebiet, weisen sie auf eine starke eo-alpidische Metamorphose im PCC hin. Weiters lässt sich eine sehr gute Übereinstimmung dieser *P-T* Daten mit den *P-T* Daten aus dem südlichen Ötztal Komplex feststellen. Dies untermauert die Annahme, dass es sich beim PCC um einen östlichen Ausläufer des Ötztal Komplexes handelt, welcher im Zuge der spät-alpinen Extension in den Ostalpen, durch die Hebung des Tauernfensters vom Ötztal Komplex getrennt wurde.

1. Introduction and geological overview

This investigation is part of a thermobarometric survey of the crystalline basement nappes north of the Tauern Window in the frame of the TRANSALP geotraverse. Since *P-T* data from this area of the Eastern Alps are almost completely lacking, obtaining these data will lead to a better understanding of the metamorphic evolution of these crystalline basement units and thus be an important contribution for the insight into the Eo-Alpine as well as pre-Alpine geological evolution of the Eastern Alps.

The polymetamorphic crystalline basement north of the Tauern Window consists of lower Ordovician porphyroid-gneisses (Kellerjochgneiss/Schwazer Augengneiss), micaschists (Patscherkofel Crystalline Complex, PCC) and Paleozoic quartzphyllites (Innsbruck Quartzphyllite Complex and Wildschönau Schists) with intercalated carbonates (Schwaz Dolomite) as shown in Figure 1. These lithologies are in a hanging wall position relative to the lithological units of the Tauern Window. In terms of its metamorphic evolution, the few geochronological data of the PCC point to a pervasive Eo-Alpine metamorphic overprint (Rockenschaub et al., 2003 b). The tectonic position of the PCC within this stack of Austroalpine nappes has been a matter of debate for some time. Tollmann (1977) attributed this crystalline nappe to be a part of the middle Austroalpine nappe complex. On the other hand, due to its higher metamorphic grade relative to the adjacent Innsbruck Quartzphyllite Complex, the PCC was thought to be part of lower Austroalpine basement nappes and thought to be the basement of the inverse lying Paleozoic phyllites of the Innsbruck Quartzphyllite (Haditsch and Mostler, 1983). In contrast, Schmidegg (1954, 1964) and Thöni (1981), thought the Patscherkofel Crystalline Complex to be an eastern remnant of the Ötztal Complex. Despite many different arguments and the still uncertain tectonic position today, no detailed petrological study of the

PCC has been performed and thus no thermobarometric data exist so far.

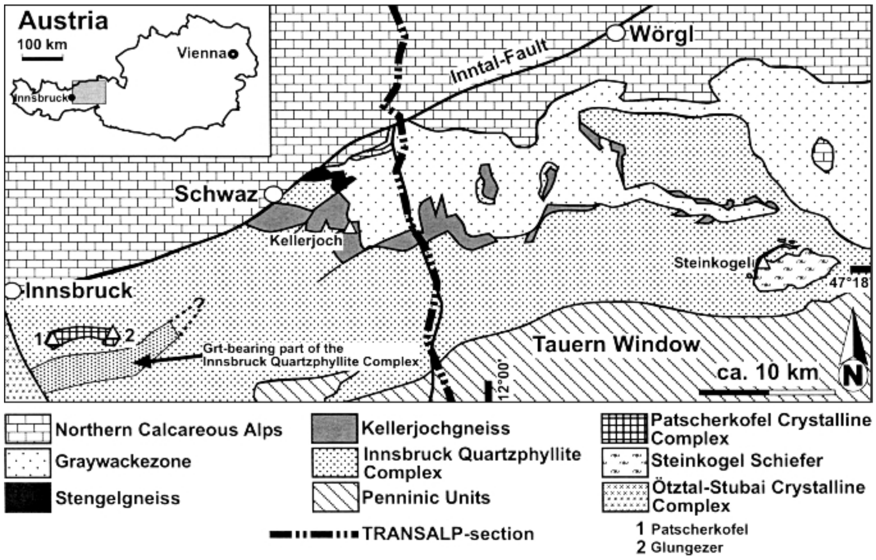

Figure 1: Geological overview of the area of investigation. Note the TRANSALP section in the center of the image crosscutting all tectonic units.

2. Lithological and petrographical description

The main part of the PCC consists of micaschists. They show alternate layering with quartzites and paragneisses (Rockenschaub et al., 2003a). Micaschists often contain garnet and staurolite porphyroblasts with diameters of up to several cm. White mica, biotite and chlorite form the penetrative foliation and pervasive folding occurs. Metabasites are intercalated within the micaschists throughout the PCC. Due to the different rheological behaviour, the metabasites are lens-shaped and laterally pinch out. They appear as dark colored amphibolites or as banded amphibolites, are very compact and show almost no foliation. The tectonic border to the rocks of the underlying Innsbruck Quartzphyllite complex consists of biotite-bearing mica schists, which are interpreted to be the thrust zone between the two units (Piber, 2005). The metapelites of the Patscherkofel Crystalline Complex contain remnants of an older (Variscan?) mineral assemblage, which is represented by staurolite, garnet$_1$ and plagioclase$_1$. During the Eo-Alpine prograde metamorphic overprint staurolite was replaced by pseudomorphs of white micas (muscovite, margarite), chloritoid and occasionally chlorite. The Eo-Alpine age of chloritoid formation has been confirmed by Rockenschaub et al. (2003b). Occasionally, corundum occurs, which seems to be in textural equilibrium with the white micas (muscovite and margarite) and chloritoid as shown in Figure 2. Textural data indicate a reaction similar to the staurolite breakdown from the southern Ötztal Crystalline as proposed by Hoinkes (1981), but in our case the anorthite component of plagioclase and the coexisting biotite also play an important role, thus enabling a model reaction such as

Staurolite + Anorthite + Biotite + H_2O = Chloritoid + Margarite + Muscovite (1)

Garnets within the metapelites often can be distinguished into two garnet generations (garnet$_1$ and garnet$_2$) as shown in Figure 3. Garnet$_2$ occurs as small rims growing around the older garnet generation, garnet$_1$. Some older garnets (garnet$_1$) contain inclusions of graphite in the core, and the number of these inclusions decreases or they are absent in the rims. Ilmenite occurs as inclusions in both garnet generations. Some garnet individuals are strongly deformed and show a skeleton-structure. Garnet$_2$ rims are occasionally replaced by chlorite due to later-stage retrogression. The mineral assemblage of the metapelites furthermore consists of muscovite, biotite, chlorite, clinozoisite and quartz. Abundant accessory minerals are zircon and titanite.

3. Mineral Chemistry

Mineral compositions were measured with a JEOL SUPERPROBE X-8100 electron microprobe at the Institute of Mineralogy and Petrography of the University of Innsbruck. Operation conditions for anhydrous minerals were 15 kV and a sample current of 20 nA, except for sheet silicates, which were measured with a reduced sample current of 10 nA and a wide beam with a diameter between 2 and 5 µm to prevent loss of alkalis. Natural and synthetic standards were used for calibration. Mineral formula calculations were performed with the programs MacAX (Holland, 1999; written comm.), NORM II (Ulmer, 1999; written comm.) and Hyperform96 (Bjerg et al., 1992).

Garnet: Garnets occur as porphyroblasts within the mica- and chlorite-rich penetrative foliation (Tab. 1). Diameters reach

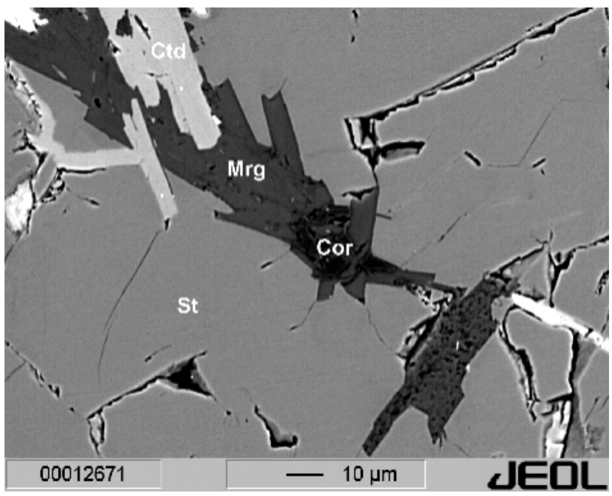

Figure 2: This BSE image shows the breakdown of staurolite (St) to chloritoid (Ctd) + margarite (Mrg) according to reaction (1) (sample PK-5). Within chloritoid, corundum (Cor) occurs.

up to 12 mm. Most of the garnets show rims, which constitute a second garnet generation, which can be seen with the polarization microscope. In backscatter electron (BSE) images the chemical difference between garnet$_1$ and garnet$_2$ can be observed, indicating a discontinuous chemical zonation (Fig. 3). Cores of garnet$_1$, which are thought to be the product of the Variscan metamorphic overprint, are almandine-rich (Alm_{72-77}). The grossular component lies between 5 and 7 mol.%. The pyrope component is slightly higher in the core (Prp_{12-14}) and decreases down to 8 mol.% in the rim of garnet$_1$. The spessartine component of garnet$_1$ lies between 12 and 14 mol.%. Garnet$_2$ forms overgrowth rims, which are the product of the Eo-Alpine metamorphic overprint. This garnet generation shows a definitely higher grossular component (Grs_{16-26}) compared to garnet$_1$, which has 5 to 7 mol.% grossular. The almandine component of garnet$_2$ is lower and shows Alm_{58-70}. The pyrope component ranges from 5 to 6 mol.% and is also distinctly lower as in garnet$_1$. The spessartine component is only slightly decreased in garnet$_2$ and varies between 10 and 14 mol.% (Fig. 4).

Sample	GLU4	GLU4	PK-5	PK-7	PK-7	PK7	PK7
	Grt_2	Grt_2	Grt_2	Grt_2	Grt_2	Grt_1	Grt_1
SiO_2	37.28	37.13	37.48	37.24	36.98	36.63	36.37
TiO_2	0.11	0.04	0.13	n.d.	n.d.	n.d.	0.04
Al_2O_3	21.12	20.82	21.22	20.31	20.36	20.66	21.11
Cr_2O_3	n.d.	n.d.	n.d.	0.06	n.d.	0.27	n.d.
Fe_2O_3	n.c.	n.c.	1.39	0.58	1.76	0.48	1.37
FeO	27.56	27.58	26.44	29.65	28.47	34.28	33.19
MnO	4.08	4.17	4.48	2.43	2.56	4.02	4.10
MgO	1.16	1.34	0.97	0.91	0.76	2.06	2.32
CaO	8.16	7.97	9.33	8.16	8.73	1.29	1.32
Na_2O	n.d.	n.d.	n.d.	0.02	0.08	n.d.	0.07
K_2O	n.d.	n.d.	0.09	0.08	0.08	0.04	0.01
Total	99.48	99.06	101.53	99.45	99.78	99.73	99.90
Si	3.001	3.005	2.966	3.016	2.987	2.986	2.952
Ti	0.007	0.002	0.008	n.d.	n.d.	n.d.	0.002
Al	2.004	1.986	1.979	1.939	1.939	1.986	2.020
Cr	n.d.	n.d.	n.d.	0.004	n.d.	0.017	n.d.
Fe^{3+}	n.c.	n.c.	0.083	0.036	0.107	0.029	0.083
Fe^{2+}	1.856	1.867	1.750	2.009	1.924	2.337	2.253
Mn	0.278	0.286	0.300	0.167	0.175	0.278	0.282
Mg	0.139	0.162	0.114	0.110	0.092	0.250	0.281
Ca	0.705	0.692	0.791	0.708	0.756	0.113	0.115
Na	n.d.	n.d.	n.d.	0.003	0.013	n.d.	0.011
K	n.d.	n.d.	0.009	0.008	0.008	0.004	0.001
Sum	7.990	8.000	8.000	8.000	8.000	8.000	8.000
Alm	0.62	0.62	0.59	0.67	0.65	0.78	0.77
Sps	0.09	0.10	0.10	0.06	0.06	0.09	0.10
Prp	0.05	0.05	0.04	0.04	0.03	0.08	0.10
Grs	0.24	0.23	0.27	0.24	0.26	0.04	0.04

Table 1: Representative electron microprobe analyses of garnet. Calculations on the base of 12 oxygen; n.d.: not detected; n.c.: not calculated; Grt_2: garnet rim analysis, Grt_1: garnet core analysis; Alm: almandine, Sps: spessartine, Prp: pyrope, Grs: grossular.

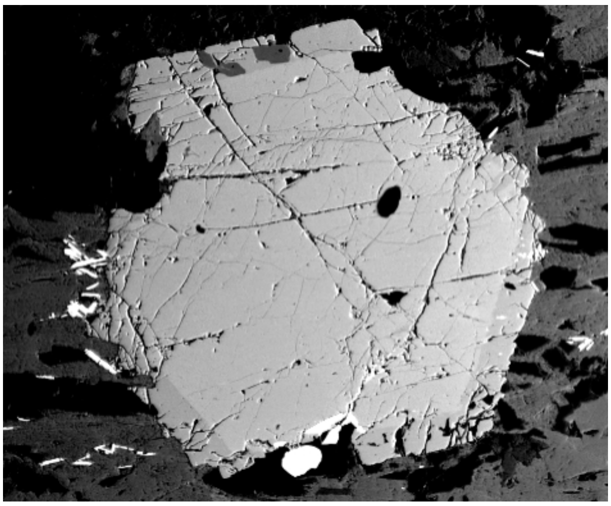

Figure 3: This BSE image shows the discontinuous zonation of a garnet of the Patscherkofel Crystalline Complex (sample PK-5). Garnet2 appears as small, darker rims surrounding garnet$_1$.

Staurolite: As a remnant of the Variscan mineral assemblage, staurolite occurs as pseudomorphs with diameters of up to several cm which are replaced by white mica (muscovite, margarite) and chloritoid. Relics of staurolite still occur in the core of the pseudomorphs. Staurolite shows $Fe^{2+}/(Fe^{2+}$ + Mg) ratios of 0.87 to 0.93 (Tab. 2). The Zn contents lie between 0.36 and 0.66 a.p.f.u. and the Mn contents are low and vary from 0.01 to 0.07 a.p.f.u.

Chloritoid is a product of the prograde Eo-Alpine overprint of staurolite. It shows Mg contents between 0.32 and 0.34 a.p.f.u. and low Mn contents between 0.02 and 0.08 a.p.f.u. (Tab. 2). The $Fe^{2+}/(Fe^{2+}$ + Mg) ranges from 0.88 to 0.90.

Margarite mainly occurs within fractures of staurolite and is also considered as a product of the prograde Eo-Alpine metamorphic overprint as well. The margarite crystals are often in textural equilibrium with chloritoid and occasionally corundum. The Ca contents vary between 0.77 and 0.84 a.p.f.u., the Na contents are in a range of 0.15 and 0.21 a.p.f.u. (Tab. 3). The K contents are very low and less than 0.02 a.p.f.u.

Muscovite is part of the matrix as well as the pseudomorphic replacement of staurolite. Matrix muscovite is aligned within the Eo-Alpine penetrative foliation. Muscovite from the staurolite pseudomorphs is sligthly more enriched in Na than matrix muscovite with Na contents ranging from 0.09 to 0.22 a.p.f.u. The Na contents of matrix muscovite are distinctly lower and lie between 0.04 and 0.09 a.p.f.u. The Si contents of both muscovite types vary between 3.06 and 3.26 a.p.f.u., where muscovite from the pseudomorphs show slightly lower Si contents (Tab. 3).

Biotite also forms part of the Eo-Alpine penetrative foliation (Tab. 4). The Fe^{2+}/Fe^{2+} + Mg ratios range from 0.50 to 0.61. The Fe^{2+} contents lie between 1.19 and 1.46 a.p.f.u. and Mg contents vary from 0.97 to 1.21 a.p.f.u. The Ti contents range from 0.11 to 0.82 a.p.f.u.

Chlorite also is part of the Eo-Alpine penetrative foliation (Tab. 4). The $Fe^{2+}/(Fe^{2+}$ + Mg) ratio ranges from 0.44 to 0.54. The Fe^{2+} contents vary from 1.98 to 2.48 a.p.f.u. and Mg contents range from 2.15 to 2.53 a.p.f.u. The Al_{tot} contents range from 2.62 to 2.74 a.p.f.u.

Plagioclase shows a discontinuous chemical zonation and chemically also occurs in two generations similar to garnet (Fig. 5). The plagioclase-rich cores (plagioclase$_1$) are thought to be of Variscan origin and show a composition of An_{22-30} Ab_{69-77} Or<$_1$. The albite-rich rim compositions (plagioclase$_2$), correspond to the later Eo-Alpine metamorphic overprint and show a feldspar composition of An_{6-10} Ab_{89-92} Or<$_1$ (Tab. 5).

4. Thermobarometry

In order to obtain *P-T* data of the Eo-Alpine peal metamorphic conditions, thermobarometry involving the assemblage plagioclase$_2$ + muscovite + biotite + chlorite + garnet$_2$ + quartz was used. For thermometry, the Fe-Mg exchange reaction between garnet and biotite was applied to equilibrium assemblages using the calibrations of Patiño-Douce (1993) and Kleeman and Reinhardt (1994). In one sample from the Patscherkofel Crystalline Complex (PK-6), the Fe-Mg exchange reaction between phengite and garnet, using the calibration models of Hynes and Forest (1988) and Krogh and Raheim (1978), was used. Pressure estimates of metapelites of the Patscherkofel Crystalline Complex were performed using the net-transfer reaction based on the equilibrium assemblage garnet$_2$ + plagioclase$_2$ + muscovite + biotite + quartz (Ghent and Stout, 1981; Powell and Holland, 1988; Hoisch, 1990). For biotite-absent mineral assemblages in sample PK-6 of the Patscherkofel Crystalline Complex the net-transfer reaction within the equilibrium assemblage garnet$_2$ + plagioclase$_2$ + muscovite + quartz (Hoisch, 1990) was applied.

Furthermore multi-equilibrium calculation methods such as THERMOCALC v.3.02 (Holland and Powell, 1998) and TWQ v.1.02 (Berman, 1988, 1992) were used. The computations with THERMOCALC in the system K_2O-CaO-Na_2O-FeO-MgO-Al_2O_3-SiO_2-H_2O (KCNFMASH), with and without H_2O (KCNF MAS), were performed with the thermodynamic data set of Holland and Powell (1998). TWQ calculations in the system K_2O-CaO-FeO-MgO-Al_2O_3-SiO_2-H_2O (KCFMASH), again with and without H_2O (KCFMAS) were done with the expanded data set Jun92.gsc (Berman, 1992, written comm.).

4.1 Cation exchange thermometers and net-transfer reactions

Application of the garnet – biotite Fe-Mg exchange thermometer and the garnet – plagioclase – muscovite – biotite barometer yields temperatures ranging between 510 and 570°C and pressures ranging from 9.5 to 12.2 kbar by using the mineral assemblage garnet$_2$ + muscovite + biotite + chlorite + plagioclase$_2$ + quartz from samples PK-5 (Fig. 6) and GLU-4. Calculations of sample PK-7 yield slightly lower pressures at 7 to 8.1 kbar and a temperature range of 515 to 538°C. The application of the garnet – phengite Fe-Mg exchange thermometer and the garnet – plagioclase – muscovite – quartz barometer for sample PK-6 resulted in pressures between 8.2 and 11.2 kbar and temperatures ranging from 497 to 570°C (Fig. 7). Variations in chemical composition of garnet, biotite and muscovite yield maximum temperature shifts of 73°C. Compositional variations of plagioclase$_2$ and muscovite are mainly responsible for pressure shifts in a range between 7.0 and

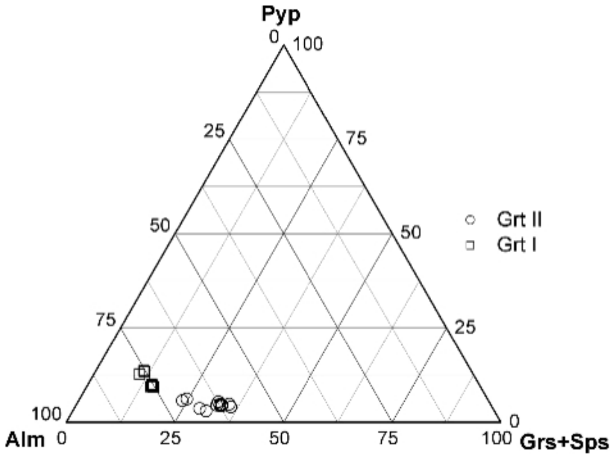

Figure 4: Plot illustrating the chemical differences between garnet$_1$ and garnet$_2$. Variscan garnet$_1$ (open squares) is enriched in the almandine component (samples PK-5, PK-7, GLU-4).

Sample	PK-1	PK-1	PK-1	PK-1	PK-1	PK-1
	Sta	Sta	Sta	Ctd	Ctd	Ctd
SiO_2	26.61	26.76	26.76	23.75	24.40	23.83
TiO_2	0.30	0.39	0.57	0.02	0.07	0.05
Al_2O_3	54.35	55.19	54.38	40.50	40.91	40.79
Cr_2O_3	n.d.	0.06	n.d.	0.08	0.15	0.02
Fe_2O_3	n.c.	n.c.	n.c.	1.24	n.c.	0.527
FeO	11.96	12.67	11.99	23.92	25.57	24.886
MnO	n.d.	0.10	0.26	0.73	0.18	0.34
MgO	0.69	0.55	0.77	1.79	1.68	1.85
CaO	0.12	n.d.	0.21	n.d.	0.04	n.d.
ZnO	3.16	1.75	2.32	n.a.	n.a.	n.a.
Na_2O	0.28	0.43	0.26	0.11	n.d.	n.d.
K_2O	n.d.	0.01	n.d.	0.02	n.d.	n.d.
Total	97.47	97.91	97.52	92.17	93.00	92.33
Si	7.486	7.457	7.502	1.979	2.013	1.981
Ti	0.063	0.082	0.12	0.001	0.004	0.003
Al	18.019	18.126	17.966	3.977	3.977	3.996
Cr	n.d.	0.013	n.d.	0.005	0.010	0.004
Fe^{3+}	n.c.	n.c.	n.c.	0.078	n.c.	0.033
Fe^{2+}	2.813	2.953	2.811	1.666	1.764	1.730
Mn	n.d.	0.023	0.061	0.052	0.013	0.024
Mg	0.289	0.229	0.322	0.222	0.207	0.230
Ca	0.036	n.d.	0.063	n.d.	0.003	n.d.
Zn	0.657	0.360	0.480	n.a.	n.a.	n.a.
Na	0.152	0.233	0.142	0.018	n.d.	n.d.
K	n.d.	0.003	n.d.	0.002	n.d.	n.d.
Fe#	0.91	0.93	0.90	0.88	0.89	0.88
Sum	29.516	29.479	29.466	8.000	7.990	8.001

Table 2: Representative electron microprobe analyses of staurolite and chloritoid.
Calculations of staurolite formulae on the base of 46 oxygen and chloritoid formulae on the basis of 12 oxygen and 8 cations; n.d.: not detected; n.c.: not calculated; n.a.: not analyzed; Sta: staurolite, Ctd: chloritoid; Fe#: $Fe^{2+}/(Fe^{2+} + Mg)$.

12.2 kbar, but most pressures lie within the range of 8.8 to 10.6 kbar.

4.2 Multi-equilibrium calculations

THERMOCALC v.3.02: Thermobarometric results from mineral equilibria in metapelitic samples of the Patscherkofel Crystalline Complex were obtained by calculation of intersections among a given set of mineral reactions calculated with the data set of Holland and Powell (1998). Due to the larger number of reactions, most *P-T* results were obtained with the H_2O-involving system KCNFMASH. In these calculations H_2O was assumed to present, but not in excess. In order to obtain *P-T* estimates, independent of a(H_2O), additional calculations were performed with the H_2O-absent system KCNFMAS. Intersections were computed by using the endmembers almandine – pyrope – grossular – phlogopite – annite - muscovite – paragonite – clinochlore – daphnite – anorthite – celadonite – quartz ± H_2O. For these calculations, only chlorite from the penetrative foliation, which is in equilibrium with muscovite and biotite, was used. Calculations in the system KCNFMASH resulted in pressures ranging from 10.1 to 11.5 kbar and temperatures between 513 and 585°C. The average standard deviation yielded 1.1 kbar in pressure (1σ) and 18°C in temperature (1σ). Calculations with the H_2O-absent system yielded lower pressures from 7.3 to 10.5 kbar with average standard deviations of 1.8 kbar (1σ) at a temperature range between 454 and 513°C with an average standard deviation of 80°C (1σ). Variations in pressure are mostly dependent on compositional variations of plagioclase$_2$ and less of muscovite. Maximum shifts of 0.5 kbar within an assemblage of one sample could be obtained by using different chemical compositions of plagioclase$_2$. Temperature shifts strongly depend on compositional variations of garnet and minor on biotite and yielded a maximum of 10°C by applying different garnet compositions within one sample.

TWQ v.1.02: *P-T* results of samples of the Patscherkofel Crystalline Complex were obtained by calculating intersections of metapelitic samples using TWQ v1.02 based on the data set of Berman (1992). Calculations were performed with the H_2O-present system KCFMASH and the H_2O-absent system KCFMAS by using the mineral assemblage garnet$_2$ + biotite + muscovite + chlorite + plagioclase$_2$ + quartz. Again, H_2O was assumed to be present but not in excess. The activities of clinochlore and daphnite were calculated with an ideal-ionic model according to Powell (1978). In addition, the ideal ionic model X_{Mg}^{5}, which only considers mixing on the octahedral sites, was applied. Since considerably mixing also takes place on the tetrahedral site, this model only represents a limiting approximation.

Calculations performed with the H_2O-involving system yield pressures in the range of 10.3 to 11.7 kbar with standard deviations reaching from 1.3 to 1.8 kbar (1σ). Temperatures range from 493 to 535°C with standard deviations ranging from 13 to 28°C (1σ). *P-T* calculations performed with the H_2O-absent system resulted in pressures ranging from 9.6 to 11.4 kbar and standard deviations between 0.3 and 1.8 kbar (1σ). Temperatures range from 471 to 493°C with standard deviations ranging from 14 to 56°C (1σ).

Variations of the activity models of chlorite (one-site vs. multi-site ionic models) resulted in a maximum pressure shifts of ± 0.2 kbar and maximum deviations in temperature of ± 7°C.

Sample	PK-1	GLU4	GLU4	PK7	PK7	PK7
	mrg	ms24	ms26	ms2	ms3	ms4
SiO_2	31.07	45.93	46.77	47.89	48.25	49.40
TiO_2	0.81	0.59	0.57	0.18	0.25	0.41
Al_2O_3	49.13	35.21	35.99	30.56	32.12	31.07
Cr_2O_3	n.d.	n.d.	n.d.	n.d.	0.02	0.02
Fe_2O_3	0.71	n.c.	n.c.	3.01	n.c.	n.c.
FeO	n.c.	1.57	1.20	1.16	1.87	2.30
MnO	n.d.	0.10	n.d.	0.02	0.02	0.01
MgO	0.09	0.72	0.64	3.18	1.76	2.02
CaO	10.78	0.03	0.03	0.18	0.01	0.01
Na_2O	1.59	1.29	1.51	0.76	0.55	0.46
K_2O	0.01	9.82	9.36	9.23	10.57	10.34
Total	94.191	95.27	96.08	96.18	95.43	96.05
Si	2.081	3.061	3.072	3.173	3.213	3.266
Ti	0.041	0.030	0.028	0.009	0.013	0.020
Al^{IV}	0.919	0.939	0.928	0.827	0.787	0.734
Al^{VI}	2.959	1.828	1.859	1.560	1.734	1.688
Cr	n.d.	n.d.	n.d.	n.d.	0.001	0.001
Fe^{3+}	0.036	n.c.	n.c.	0.150	n.c.	n.c.
Fe^{2+}	n.c.	0.088	0.066	0.064	0.104	0.127
Mn	n.d.	0.006	0.000	0.001	0.001	0.001
Mg	0.009	0.072	0.063	0.314	0.175	0.199
Ca	0.774	0.002	0.002	0.013	0.001	0.001
Na	0.206	0.167	0.192	0.098	0.071	0.059
K	0.001	0.836	0.785	0.781	0.899	0.873
Sum	7.025	7.027	6.995	6.989	6.998	6.968

Table 3: Representative electron microprobe analyses of margarite and muscovite.
Calculations on the base of 11 oxygen, n.d.: not detected; n.c.: not calculated; mrg: margarite; ms24, ms26: muscovites from staurolite pseudomorphs; ms2, ms3, ms4: matrix muscovites.

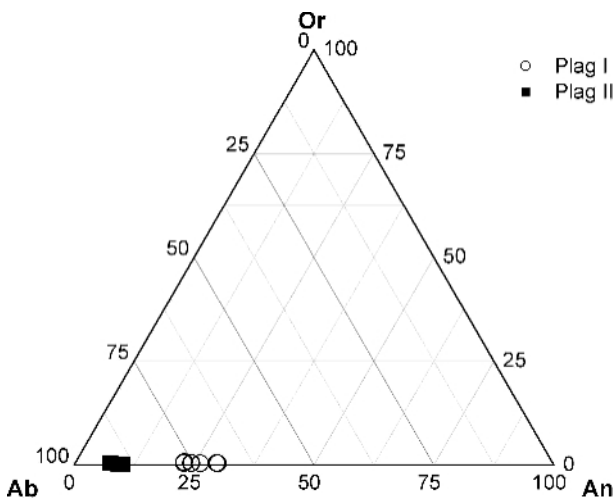

Figure 5: This triangle plot illustrates the chemical composition of the feldspars from the Patscherkofel Crystalline Complex. Two different plagioclase generations can be observed, whereby plagioclase1 (open circles) is enriched in anorthite component (samples PK-5, GLU-4, PK-7).

Pressure variations are mostly due to compositional differences in garnet$_2$, plagioclase and muscovite, and considering the mineral assemblages in one sample, they are in a maximum range of 0.3 kbar. Temperature shifts mostly depend on Fe-Mg exchange reactions and thus the compositional variation of garnet$_2$, biotite and chlorite and are in a maximum range of 11°C per sample.

Sample	GLU4	PK-5	PK7	PK7	GLU4	PK-5	PK7
	bt20	bt3	bt1	bt2	chl29	chl1	chl2
SiO_2	36.58	35.99	36.46	37.11	25.23	25.11	26.34
TiO_2	1.87	1.60	1.54	1.63	0.05	n.d.	0.09
Al_2O_3	17.58	18.77	19.02	18.63	21.92	21.33	22.07
Cr_2O_3	n.d.	0.11	0.11	0.08	n.d.	0.03	0.03
Fe_2O_3	n.c.	0.09	n.c.	n.c.	n.c.	n.c.	n.c.
FeO	20.94	20.86	19.44	19.01	26.63	25.75	23.08
MnO	0.11	0.28	0.10	0.09	0.13	0.23	0.11
MgO	9.08	9.16	10.35	10.79	13.67	13.79	16.75
CaO	0.09	0.10	0.08	0.04	n.d.	0.12	0.05
Na_2O	0.12	0.21	0.19	0.18	0.03	0.04	0.02
K_2O	8.98	8.33	8.77	8.77	0.02	n.d.	0.05
Total	95.36	95.51	96.07	96.34	87.68	86.40	88.59
Si	2.791	2.735	2.735	2.766	2.674	2.695	2.705
Ti	0.107	0.091	0.087	0.091	0.004	n.d.	0.007
Al^{IV}	1.209	1.265	1.265	1.234	1.326	1.305	1.295
Al^{VI}	0.373	0.416	0.417	0.403	1.413	1.394	1.377
Cr	n.d.	0.007	0.007	0.005	n.d.	0.003	0.002
Fe^{3+}	n.c.	0.005	n.c.	n.c.	n.c.	n.c.	n.c.
Fe^{2+}	1.336	1.325	1.220	1.185	2.360	2.312	1.982
Mn	0.007	0.018	0.006	0.006	0.012	0.021	0.010
Mg	1.033	1.037	1.157	1.199	2.159	2.206	2.563
Ca	0.007	0.008	0.006	0.003	n.d.	0.014	0.006
Na	0.018	0.031	0.028	0.026	0.006	0.008	0.004
K	0.875	0.808	0.840	0.835	0.003	n.d.	0.007
Fe#	0.56	0.56	0.51	0.50	0.52	0.51	0.56
Sum	7.757	7.747	7.768	7.752	9.957	9.958	9.957

Table 4: Representative electron microprobe analyses of biotite and chlorite.
Calculations on the base of 11 oxygen; n.d.: not detected; n.c.: not calculated; bt: biotite, chl: chlorite; Fe#: $Fe^{2+}/(Fe^{2+} + Mg)$.

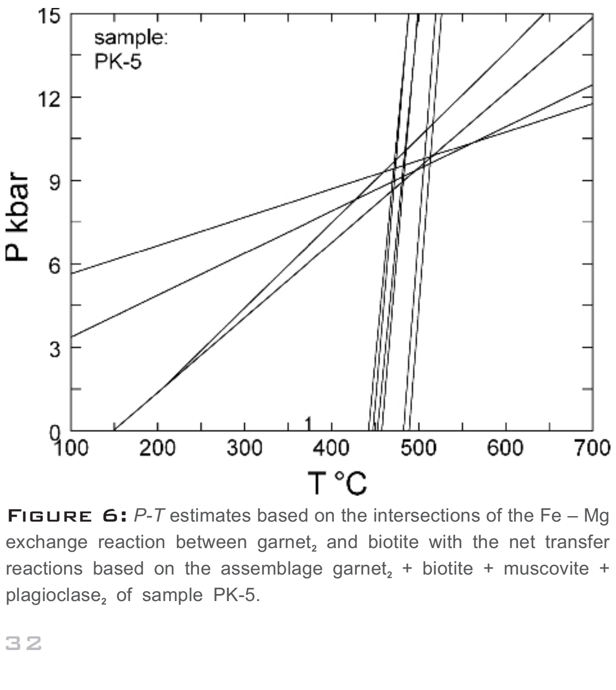

Figure 6: *P-T* estimates based on the intersections of the Fe – Mg exchange reaction between garnet$_2$ and biotite with the net transfer reactions based on the assemblage garnet$_2$ + biotite + muscovite + plagioclase$_2$ of sample PK-5.

5. Discussion

Thermobarometric results of the Patscherkofel Crystalline Complex reveal a totally different metamorphic overprint compared to most of the surrounding lithologies of the Innsbruck Quartzphyllite Complex. The Variscan amphibolite-facies mineral assemblage staurolite + garnet$_1$ + plagioclase$_1$ and the Eo–Alpine paragenesis garnet$_2$ + biotite + muscovite + chlorite + plagioclase$_2$ + quartz ± margarite ± chloritoid indicate a similar polymetamorphic evolution as the metapelitic rocks from the neighboring Ötztal Complex (e.g. Tropper and Recheis, 2003) and the Ortler-Campo Crystalline Complex further south (e.g. Mair et al., 2006). Unfortunately, due to the lack of appropriate Variscan mineral assemblages, it was not possible to calculate the *P-T* conditions of the Variscan metamorphic overprint.

Thermobarometric constraints of the Eo-Alpine mineral assemblage garnet$_2$ + muscovite + biotite + chlorite + plagioclase$_2$ + quartz were obtained applying Fe – Mg cation exchange thermometry and net-transfer reactions which resulted in a pressure range of 9.5 to 12.2 kbar at a temperature range between 510 and 570°C for most of the samples (Figs. 6, 7). Therefore our investigation yields similar *P-T* conditions for the Eo-Alpine metamorphic overprint as chloritoid-bearing samples from the Ötztal Complex (Tropper and Recheis, 2003).

Petrological and thermobarometric investigations of the PCC imply the polymetamorphic nature of this basement complex (Variscan and Eo-Alpine), which is in agreement with geochronological data from the PCC by Rockenschaub et al. (2003b) which range from 180 Ma to 106 Ma. The *P-T* estimates are indicative for a temperature-accentuated amphibolite-facies metamorphic event during the Variscan and an Eo-Alpine metamorphic overprint under *P*-accenuated high greenschist- to epidote-amphibolite-facies conditions. These results cannot be correlated to the lithologies of the Innsbruck Quartzphyllite Complex, except the biotite-bearing micaschists beneath the tectonic border with the PCC, which yields similar *P-T* results and are thought to be part of the Innsbruck Quartzphyllite Complex (Piber, 2002). The Eo-Alpine *P-T* constraints of the Patscherkofel Crystalline Complex also do not correspond to the low P-T results from the NE part of the Ötztal Complex underneath the Kalkkögel nappe, which yield pressures of 3.7 to 4.2 kbar at temperatures of 469 to 485°C (Tropper and Recheis, 2003). On the other hand, the *P-T* results are in good agreement with the thermobarometric constraints of the Schneeberg Complex and the southernmost Ötztal Complex at pressures of 9 to 12 kbar and a temperature of 580°C (Hoinkes, 1986; Konzett and Hoinkes, 1991, 1996; Exner et al., 2001; Habler et al., 2001; Konzett and Tropper, 2001; Tropper and Recheis, 2003). The discrepancy of the thermobarometrical estimates of the Patscherkofel Crystalline Complex compared to results of the neighboring middle and northern Ötztal Complex might be an effect of vertical displacement induced by the Brenner fault zone.

The *P-T* estimates of the PCC are in contrast to the results of several authors (Tollmann, 1986; Steyrer and Finger, 1996), who considered the PCC and the Kellerjochgneiss to be part of the same crystalline complex. The mineral assemblages and the thermobarometric data unambiguously suggest a correlation to the southern Ötztal Complex, where Tropper and Recheis (2003) described similar mineral assemblages and metamorphic conditions. The $garnet_2$ composition of the Patscherkofel Crystalline Complex reveals the typical Ca-rich chemical composition for the Eo-Alpine metamorphism according to compositional similarity of garnets from Ötztal Complex (Tropper and Recheis, 2003). The biotite micaschists and the overlying Patscherkofel Crystalline Complex must be regarded as separate crystalline fragments separated from the Innsbruck Quartzphyllite Complex. In evidence of structural and metamorphic conditions Schmid et al. (2004) simplify the geotectonic position of crystalline basement nappes in the north of the Tauern Window. In consequence they attribute the Innsbruck Quartzphyllite Complex, the Kellerjochgneiss and the Greywacke Zone with its sedimentary cover to the upper Austroalpine units, thus representing the lower plate. On the other hand, the crystalline basement nappe in the west of the Tauern Window (Ötztal Complex) is attributed to the upper plate. According to the tectonic model by Schmid et al. (2004) and due to comparable metamorphic evolution and mineral paragenesis, the Patscherkofel Crystalline Complex can be attributed to the upper plate and would suggest the Patscherkofel Complex to be part of the basis of the Ötztal Complex. The biotite-micaschists underneath it, which display similar *P-T* conditions as the Patscherkofel Crystalline might therefore represent a metamorphic thrust zone between the Patscherkofel Crystalline Complex and the Innsbruck Quartzphyllite and marks the borderline between the tectonically upper plate and the lower plate. The remaining underlying Innsbruck Quartzphyllite lithologies beneath these crystalline fragments would therefore be attributed to be part of the lower plate.

Similar thermobarometric estimates from the neighboring Ötztal Complex suggest the Patscherkofel Crystalline Complex to be a crystalline fragment of the Ötztal Complex, which has been thrusted onto the Innsbruck Quartzphyllite Complex after the peak of Eo-Alpine metamorphism. Latter is confirmed by geochronological data by Rockenschaub et al. (2003b), who obtained ages of 51 Ma and 71 Ma for diaphtoritic, mylonitic gneisses from the basis of the PCC.

Sample	GLU4	PK7	PK7	PK-7	PK-7	PK-6
	$Plag_2$	$Plag_2$	$Plag_2$	$Plag_1$	$Plag_1$	$Plag_1$
SiO_2	68.37	66.33	67.00	60.57	61.22	63.07
TiO_2	0.03	0.01	n.d.	n.d.	0.03	0.08
Al_2O_3	20.69	22.10	21.56	23.88	25.01	23.80
Cr_2O_3	0.00	n.d.	n.d.	n.d.	n.d.	n.d.
Fe_2O_3	0.26	0.11	0.30	0.21	0.20	0.76
FeO	n.c.	n.c.	n.c.	n.c.	n.c.	n.c.
MnO	n.d.	0.01	n.d.	0.04	n.d.	0.03
MgO	n.d.	n.d.	n.d.	n.d.	n.d.	n.d.
CaO	1.24	2.54	1.96	5.17	6.22	4.81
Na_2O	11.14	10.47	10.77	9.70	8.18	9.02
K_2O	0.05	0.07	0.02	0.08	0.09	0.13
Total	101.78	101.64	101.61	99.65	100.95	101.70
Si	2.943	2.871	2.897	2.713	2.697	2.754
Ti	0.001	0.000	0.000	0.000	0.001	0.003
Al	1.050	1.128	1.099	1.261	1.299	1.225
Cr	n.d.	n.d.	n.d.	n.d.	n.d.	n.d.
Fe^{3+}	0.008	0.004	0.010	0.007	0.007	0.025
Fe^{2+}	n.c.	n.c.	n.c.	n.c.	n.c.	n.c.
Mn	n.d.	n.d.	n.d.	0.002	n.d.	0.001
Mg	n.d.	n.d.	n.d.	n.d.	n.d.	n.d.
Ca	0.057	0.118	0.091	0.248	0.294	0.225
Na	0.930	0.879	0.903	0.842	0.699	0.764
K	0.003	0.004	0.001	0.005	0.005	0.007
Sum	4.993	5.004	5.001	5.077	5.002	5.004
An	0.06	0.12	0.09	0.23	0.29	0.23
Ab	0.94	0.88	0.91	0.77	0.70	0.77
Kfs	0.00	0.00	0.00	0.00	0.01	0.01

TABLE 5: Representative electron microprobe analyses of feldspar. Calculations on the base of 8 oxygen; n.d.: not detected; n.c.: not calculated; An: anorthite; Ab: albite; Kfs: K-feldspar; $Plag_2$: rim analysis; $Plag_1$: core analysis.

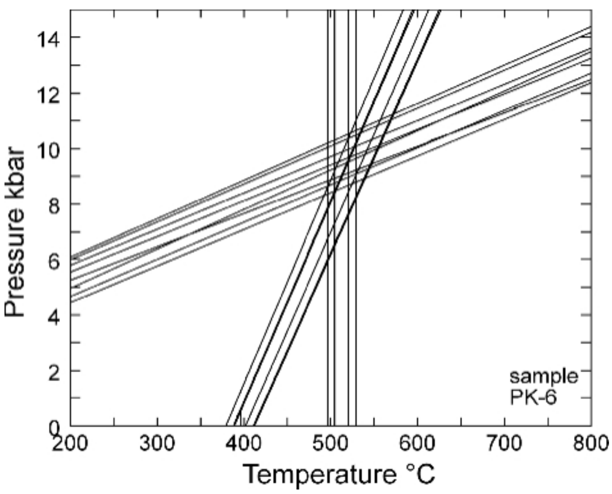

FIGURE 7: *P-T* estimates of sample PK-6 based on the Fe – Mg exchange reactions between $garnet_2$ and phengite and $garnet_2$ and biotite and the net transfer reaction $garnet_2$ – muscovite – $plagioclase_2$ – quartz.

ACKNOWLEDGMENTS

The authors wish to thank the FWF for financial support in the course of project P14571-B06 (to P.M.). Edgar Mersdorf and Bernhard Sartory are thanked for their help with the electron microprobe. The manuscript was considerably improved by the constructive reviews of Péter Horváth and Veronika Tenczer. Bernhard Grasemann is thanked for the editorial handling.

References

Berman, R.G., 1988. Internally-consistent thermodynamic data for minerals in the system SiO_2-K_2O-Na_2O-Fe_2O_3-TiO_2-Al_2O_3-FeO-MgO-K_2O-H_2O-CO_2. Journal of Petrology, 29, 445-522.

Bjerg, S.C., Mogessie, A. and Bjerg, E., 1992. Hyper Form-A hypercard program for the Mac Intosh microcomputers to calculate mineral formulae from electron microprobe and wet chemical analyses, Computers and Geoscience, 18, 717-745.

Exner, U., Fusseis, F., Grasemann, B., Habler, G., Linner, M., Sölva, H., Thiede, R. and Thöni, M., 2001. Cretaceous eclogite-facies metamorphism in the Eastern Alps: New insights, data and correlations from an interdisciplinary study. Journal of Conference Abstracts, 6/1, 387.

Ghent, E.D. and Stout, M.Z., 1981. Metamorphism at the base of the Samail Ophiolite, southeastern Oman mountains. Journal of Geophysical Research, 86, B4, 2557 2571.

Habler, G., Linner, M., Thiede, R. and Thöni, M., 2001. Eo-Alpine andalusite in the Schneeberg Complex (Eastern Alps, Italy/Austria): Constraining the P-T-t-D path during Cretaceous Metamorphism. Journal of Conference Abstracts, 6, 340.

Haditsch, G. and Mostler, H., 1983. The succession of ore mineralization of the lower Austroalpine Innsbruck quartz phyllite. In: Schneider, H. J., (ed.), Mineral deposits in the Alps, Springer Verlag, Berlin-Heidelberg-New York, pp. 1-40.

Hoinkes, G., 1986. Effect of grossular-content in garnet on the partitioning of Fe and Mg between garnet and biotite. Contributions to Mineralogy and Petrology, 92, 393-399.

Hoinkes, G., 1981. Mineralreaktionen und Metamorphosebedingungen in Metapeliten des westlichen Schneebergerzuges und des angrenzenden Altkristallins. Tschermaks Mineralogische Petrographische Mitteilungen, 28, 31-54.

Hoisch, T.D., 1990. Empirical calibration of six geobarometers for the mineral assemblage quartz + muscovite + biotite + plagioclase + garnet. Contributions to Mineralogy and Petrology, 104, 225-234.

Holland, T.J.B. and Powell, R., 1998. An internally-consistent thermodynamic data set for phases of petrological interest. Journal of Metamorphic Geology, 8, 89-124.

Hynes, A. and Forest, R.C., 1988. Empirical garnet-muscovite geothermometry in low-grade metapelites, Selwyn Range (Canadian Rockies), Journal of Metamorphic Geology, 6, 297-309.

Kleemann, J. and Reinhardt, J., 1994. Garnet-biotite thermometry revisited: The effect of Al(VI) and Ti in biotite. European Journal of Mineralogy, 6, 925-941.

Konzett, J. and Hoinkes, G., 1991. High pressure metamorphism in the Austroalpine Schneeberg Complex and adjacent Ötztal basement rocks. Terra Abstracts, 3, 88.

Konzett, J. and Hoinkes, G., 1996. Paragonite – hornblende assemblages and petrological significance: an example from the Austroalpine Schneeberg Complex, Southern Tyrol, Italy. Journal of Metamorphic Geology, 14, 85-101.

Konzett, J. and Tropper, P., 2001. Petrology of an unusual Ca-amphibole + staurolite bearing amphibolite and its implications for the high pressure metamorphism in the Schneeberg Complex, Eastern Alps. Geologisch-Paläontologische Mitteilungen der Universität Innsbruck, 25, 126.

Krogh, E.J. and Råheim, A., 1978. Temperature and pressure dependence of Fe-Mg partitioning between garnet and phengite, with particular reference to eclogites. Contributions to Mineralogy and Petrology, 66, 75-80.

Mair, V., Tropper, P. and Schuster, R., 2006. The P-T-t evolution of the Ortler-Campo Crystalline (South-Tyrol/Italy). PANGEO 2006, Innsbruck University Press, 186-187.

Patiño Douce, A.E., 1993. Titanium substitution in biotite: an empirical model with applications to thermometry, O_2 and H_2O barometries, and consequences for biotite stability. Chemical Geology, 108, 133-162.

Piber, A., 2002. Tectonometamorphic evolution of the Austro-Alpine nappes in the northern Zillertal-Area, Eastern Alps. Masters Thesis, University of Innsbruck, Innsbruck, 268 pp.

Powell, R., 1978. Equilibrium Thermodynamics in Petrology. Harper and Row, London. 284 pp.

Powell, R. and Holland, T.J.B., 1988. An internally consistent thermodynamic data set with uncertainties and correlations: 3. Application methods, worked examples and a computer program. Journal of Metamorphic Geology, 6, 173-204.

Rockenschaub, M., Kolenprat, B. and Nowotny, A., 2003a. Innsbrucker Quarzphyllitkomplex, Tarntaler Mesozoikum, Patscherkofelkristallin. Arbeitsberichte zur Arbeitstagung der Geologischen Bundesanstalt in Trins im Gschnitztal 2003, 41-58.

Rockenschaub, M., Kolenprat, B. and Frank, W., 2003b. Geochronologische Daten aus dem Brennergebiet: Steinacher Decke, Brennermesozoikum, Ötz-Stubai-Kristallin, Innsbrucker Quarzphyllitkomplex, Tarntal Mesozoikum. Arbeitsberichte zur Arbeitstagung der Geologischen Bundesanstalt in Trins im Gschnitztal 2003, 117-124.

Schmid, S.M., Fügenschuh, B., Kissling, E. and Schuster, R. 2004. Tectonic map and overall architecture of the Alpine orogen, Eclogae Geologae Helveticae, 97/1, 93-117.

Schmidegg, O., 1954. Achsen- und Flächengefüge beiderseits des Silltalbruches zwischen Innsbruck und Matrei, Tschermaks Mineralogische und Petrographische Mitteilungen, 4, 125-137.

Schmidegg, O., 1964. Die Ötztaler Schubmasse und ihre Umgebung. Verhandlunger der Geologischen Bundesanstalt, 1957/1, 76-77.

Steyrer, H.P. and Finger, F., 1996. Der Schwazer Augengneis: ein östlicher Ausläufer des Ötztal Kristallins? Mitteilungen der Österreichischen Mineralogischen Gesellschaft, 141, 226-227.

Thöni, M., 1981. Degree and evolution of the Alpine metamorphism in the Austroalpine unit W of the Hohe Tauern in the light of K/Ar and Rb/Sr age determinations on micas. Jahrbuch der geologischen Bundesanstalt, 124, 111-174.

Tollmann, A., 1963. Ostalpensynthese, Franz Deuticke, Vienna, 256 pp.

Tollmann, A., 1977. Geologie von Österreich, Bd.1, Die Zentralalpen, Franz Deuticke, Vienna, 766 pp.

Tollmann, A., 1986. Geologie von Österreich, Bd.3., Gesamtübersicht, Franz Deuticke, Vienna, 718 pp.

Tropper, P. and Recheis, A., 2003. Garnet zoning as a window into the metamorphic evolution of a crystalline complex: the northern and central Austroalpine Ötztal-Complex as a polymorphic example. Mitteilungen der Österreichischen Mineralogischen Gesellschaft, 94 (2001), 27-53.

Received: 03. March 2008
Accepted: 30. May 2008

Andreas PIBER, Peter TROPPER*) & Peter W. MIRWALD

Institute of Mineralogy and Petrography, Faculty of Geo- and Atmospheric Sciences, University of Innsbruck, Innrain 52, A-6020 Innsbruck, Austria.

*) Corresponding author, peter.tropper@uibk.ac.at